



# Synthesis and photovoltaic properties of novel C<sub>60</sub> bisadducts based on benzo[2,1,3]-thiadiazole



Wangqiao Chen<sup>a,b</sup>, Qian Zhang<sup>c</sup>, Teddy Salim<sup>a</sup>, Sandy Adhitia Ekahana<sup>d</sup>,  
Xiangjian Wan<sup>c</sup>, Tze Chien Sum<sup>d</sup>, Yeng Ming Lam<sup>a</sup>, Alfred Hon Huan Cheng<sup>d</sup>,  
Yongsheng Chen<sup>c,\*</sup>, Qichun Zhang<sup>a,b,\*</sup>

<sup>a</sup>School of Materials Science and Engineering, Nanyang Technological University, 50 Nanyang Avenue, Singapore 639798, Singapore

<sup>b</sup>Institute for Sports Research, Nanyang Technological University, 50 Nanyang Avenue, Singapore 639798, Singapore

<sup>c</sup>Institute of Functional Polymer Materials, Center for Nanoscale Science & Technology, Nankai University, Tianjin 300071, PR China

<sup>d</sup>School of Physical and Mathematical Sciences, Nanyang Technological University, 21 Nanyang Link, Singapore 637371, Singapore

## ARTICLE INFO

### Article history:

Received 19 November 2013

Received in revised form 6 January 2014

Accepted 13 January 2014

Available online 19 January 2014

### Keywords:

Photovoltaic

C<sub>60</sub>

Solar cell acceptor

Benzo[2,1,3]thiadiazole

## ABSTRACT

A novel C<sub>60</sub> solar cell acceptor (BTOQC, benzo[2,1,3]-thiadiazole-*o*-quinodimethane-C<sub>60</sub> bisadducts) based on benzo[2,1,3]thiadiazole has been synthesized as model to study how the thiadiazole group will affect the device performance in bulk heterojunction organic photovoltaics (BHJ-OPV) with poly(3-hexylthiophene) (P3HT) as donor. The optoelectronic, electrochemistry, and photovoltaic properties of the novel bisadduct BTOQC have been fully investigated. The best device performance of this fullerene derivative in our research was obtained as 2.50% with a high V<sub>oc</sub> of 0.74 V.

© 2014 Elsevier Ltd. All rights reserved.

## 1. Introduction

Organic solar cells (OSCs) have become one of the most active research areas due to their promising advantages, such as simple structure, clean and renewable energy source, low cost, light weight, and mechanical flexibility.<sup>1–4</sup> Normally, an OSC consists of a photoactive blend layer (this layer is typically made of conjugated polymers as donors and fullerene derivatives or other molecules as acceptors), which is sandwiched between a transparent indium-tin-oxide (ITO) electrode and a low work function metal electrode. Although several strategies, such as control of the morphology of active layer,<sup>5–8</sup> modification of the electrode<sup>9,10</sup> and adjustment of donor-to-acceptor ratio,<sup>11</sup> have been strongly addressed in the past decades, the fundamental driving force to obtain higher PCE (Power Conversion Efficiency) is still laid on the design and synthesis of novel donors and acceptors.<sup>12</sup>

For donor materials, greater successes have been witnessed in the syntheses of novel materials with broad light absorptions, low bandgaps, high hole mobilities, and finely-tuned electronic energy levels.<sup>13–18</sup> However, the research progress in new acceptors is

relatively slow. Although [6,6]-phenyl-C<sub>61</sub>-butyric acid methyl ester (PC<sub>61</sub>BM) has been widely used in OSCs due to its high electron mobility and compatibility with various conjugated polymer/small molecule donor materials,<sup>19</sup> there are several limitations associated with PC<sub>61</sub>BM compound: (a) PC<sub>61</sub>BM has weak absorption in the visible region;<sup>20</sup> (b) the *Lowest-Unoccupied Molecular Orbital* (LUMO) energy level of PC<sub>61</sub>BM is relatively low when it is used in the OSCs based on the conjugated donor with a higher *Highest-Occupied Molecular Orbital* (HOMO) energy level; (c) PC<sub>61</sub>BM has high crystallinity, which may readily promote inter-molecular aggregation;<sup>21–23</sup> and (d) the interaction between PC<sub>61</sub>BM and conjugated donors is typically weak due to the lack of any functional groups on C<sub>60</sub>. To address these limitations, one strategy is to modify C<sub>60</sub> acceptor with functional groups to widen the absorption in the visible range and to enhance the whole absorption of the device. For instance, PC<sub>71</sub>BM-based OSCs usually exhibits higher PCE than PC<sub>61</sub>BM in the same condition due to the stronger absorption in the visible region.<sup>24</sup> Recently, Mikroyannidis et al.<sup>25,26</sup> replaced the methoxy (–OMe) group of the PC<sub>61</sub>BM with 4-nitro-4'-hydroxy- $\alpha$ -cyanostilbene and found that the PCE could be increased from 2.93% to 5.25%. Another way is to increase the LUMO energy level of the acceptor materials through multi-functionalization, which can desirably increase the open-circuit

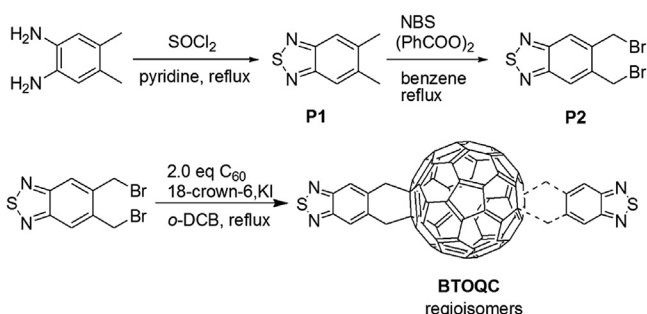
\* Corresponding authors. E-mail address: [qc Zhang@ntu.edu.sg](mailto:qc Zhang@ntu.edu.sg) (Q. Zhang).

voltage ( $V_{oc}$ ) of OSCs device because  $V_{oc}$  is proportionally determined by the difference between the LUMO energy level of the acceptor and the HOMO energy level of the donor.<sup>27</sup> Recently, a series of fullerene derivatives with higher LUMO levels than PC<sub>61</sub>BM have been employed as acceptors and poly(3-hexylthiophene) (P3HT) as the donor under 1 sun illumination in OSCs to give promising results. For instances, Lenes et al.<sup>28,29</sup> used a new [60]PCBM bisadduct (bis-PCBM) (whose LUMO level is 0.1 eV higher than that of PC<sub>61</sub>BM) as acceptor and P3HT as donor in OSCs, resulting in  $V_{oc}$  and PCE of 0.73 V and 4.5%, respectively, which are much higher than  $V_{oc}$  (0.58 V) and PCE (3.4%) of the P3HT:PC<sub>61</sub>BM-based solar cell prepared under the same conditions. He et al.<sup>30</sup> also reported a new indene-functionalized C<sub>60</sub> bisadduct (ICBA), whose LUMO energy level is 0.17 eV higher than PC<sub>61</sub>BM. The optimized OSCs based on P3HT:ICBA have a high  $V_{oc}$  (0.84 V) with a PCE as high as 6.48%. Other successful examples, such as dihydronaphthyl-C<sub>60</sub> bisadduct (NCBA), dihydronaphthyl-C<sub>70</sub> bisadduct (NC<sub>70</sub>BA), thieno-*o*-quinodimethane-C<sub>60</sub> (bis-TOQC) and di(4-methylphenyl)-methano-C<sub>60</sub> bisadduct (DMPCBA) have also been reported.<sup>31–35</sup>

Although the remarkable progress in bisadduct fullerene system has been made, there is still plenty of room for developing new efficient acceptors through reasonable chemical functionalization of fullerene. One promising strategy is to introduce the special functional groups to generate the suitable interaction (e.g., S...S interaction) between the donor and acceptor to adjust the packing or to render the separation of electron and hole more readily within the interface.<sup>36–39</sup> In this work, we design and synthesize a novel benzo[2,1,3]thiadiazole-containing fullerene derivative (benzo[2,1,3]thiadiazole-*o*-quinodimethane-C<sub>60</sub> bisadducts-(BTOQC)) through the Diels–Alder reaction to study how the hetero-atom (sulfur atom) on the acceptor will affect the final device performance. Meanwhile, the investigation on the synergistic influence of the LUMO energy levels and the absorbance on the final photovoltaic performance of the fullerene acceptors are also discussed. Our OSCs based on P3HT:BTOQC can show a reasonable PCE of 2.50% with a high  $V_{oc}$  of 0.74.

## 2. Results and discussion

The Diels–Alder reaction of fullerene provides a powerful method for fullerene functionalization.<sup>40,41</sup> The synthetic route of BTOQC is shown in Scheme 1. The synthetic route of BTOQC is shown in Scheme 1. The 5,6-bis(bromomethyl)benzo[2,1,3]thiadiazole was used as the precursors for benzo[2,1,3]thiadiazole-*o*-quinodimethane dienes and prepared according to the literature.<sup>42,43</sup> BTOQC was prepared through the [2+4] cycloaddition reaction of C<sub>60</sub> and the in situ generated benzo[2,1,3]thiadiazole-*o*-quinodimethane dienes by a published method.<sup>44,45</sup> We employed 2 equiv of precursor for the reactions in order to render the BTOQC as the main product. The yield for bisadduct BTOQC is 33%.



Scheme 1. Synthetic route of BTOQC.

The UV–vis spectra of BTOQC and the reference PC<sub>61</sub>BM are shown in Fig. 1. Both fullerene derivatives display a strong UV absorption from 200 to 350 nm in chloroform, while BTOQC shows an additional enhanced absorption in the 380–500 nm range. Much same as the UV–vis absorption of P3HT:PC<sub>61</sub>BM (Fig. S5), the solid-state absorption of P3HT:BTOQC film shows the features of both components. After annealing, the maximum absorption peak of the P3HT:BTOQC blend red-shifts for about 25 nm and shoulders at 545 and 600 nm becomes more pronounced, indicating that the heat treatment enhances P3HT crystallinity. The red-shifted absorption of the blend may contribute to the improvement of the device performance.

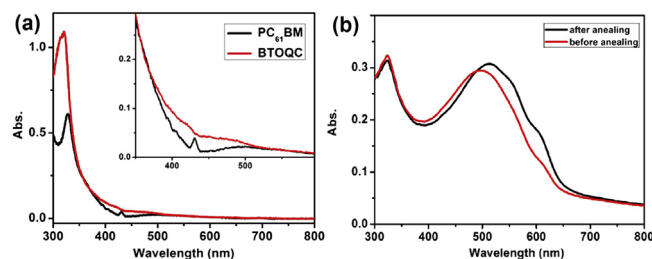


Fig. 1. UV–vis absorption spectra for: (a) BTOQC and PC<sub>61</sub>BM in chloroform ( $10^{-5}$  mol/L); (b) thin film of mixture of P3HT and BTOQC.

In Fig. 2, The DSC measurement indicates that there is no crystallization transition below 350 °C for BTOQC, while PC<sub>61</sub>BM has crystallization peaks at ca. 245 °C and 283 °C. Thus it is expected that this new acceptor is able to overcome thermally driven crystallization and achieve high thermal stability in the as-fabricated OSCs.

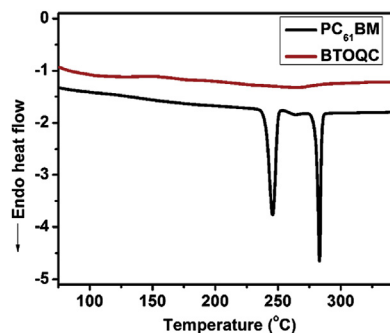
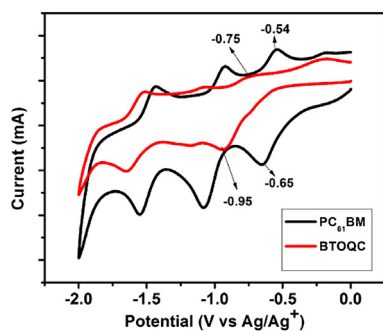


Fig. 2. Differential scanning calorimetry (DSC) measurement of BTOQC.

The electrochemical properties of BTOQC were studied by cyclic voltammetry (CV). Fig. 3 shows the CV of BTOQC as well as that of PC<sub>61</sub>BM for comparison. Both BTOQC and PC<sub>61</sub>BM exhibit three quasi-reversible reduction waves in the negative potential range from 0 to  $-2.0$  V versus Ag/Ag<sup>+</sup>. Table 1 lists the half-wave potentials (defined as  $E = 0.5[E_{p,c} + E_{p,a}]$ , where  $E_{p,c}$  is the cathodic peak potential and  $E_{p,a}$  the corresponding anodic peak potential) of the reduction processes of the fullerene derivatives BTOQC and PC<sub>61</sub>BM for comparison. It can be clearly observed that the first ( $E_1$ ), second ( $E_2$ ) and third ( $E_3$ ) reduction potentials of BTOQC all shifted negatively compared to those of PC<sub>61</sub>BM, and the onset reduction potential of BTOQC ( $-0.75$  V) is also negatively shifted compared to PC<sub>61</sub>BM ( $-0.54$  V). Moreover, the LUMO energy levels of the fullerene derivatives can be calculated from the onset reduction potentials ( $E_{red}^{on}$ ) according to the following equation,<sup>46</sup>

$$E_{LUMO} = -e(E_{red}^{on} + 4.71) [eV]$$



**Fig. 3.** Cyclic voltammograms of PC<sub>61</sub>BM and BTOQC in *o*-dichloro-benzene-acetonitrile (5:1 v/v) with 0.1 M Bu<sub>4</sub>NPF<sub>6</sub> at 100 mV/s.

**Table 1**  
Electrochemical properties of BTOQC and PC<sub>61</sub>BM

Acceptor	$E_1$ [V]	$E_2$ [V]	$E_3$ [V]	$E_{\text{red}}^{\text{on}}$ [V]	LUMO
PC <sub>61</sub> BM	-0.60	-1.00	-1.50	-0.54	-4.17
BTOQC	-0.82	-1.15	-1.60	-0.75	-3.96

where the unit of  $E_{\text{red}}^{\text{on}}$  is V versus Ag/Ag<sup>+</sup>. With this equation, the LUMO energy levels of BTOQC and PC<sub>61</sub>BM are calculated as -3.96 and -4.17 eV, respectively. Obviously, the LUMO level of BTOQC is increased by ca. 0.21 eV in comparison with that of PC<sub>61</sub>BM. Undoubtedly, the higher LUMO energy level of BTOQC is desirable for its application as an acceptor in P3HT-based OSCs because it is expected to increase the open-circuit voltage of the devices.

To evaluate the new BTOQC acceptor, bulk heterojunction solar cells based on the ITO/PEDOT:PSS/P3HT:Acceptor/LiF/Al configuration were fabricated and characterized under simulated 100 mW/cm<sup>2</sup> AM 1.5 G illumination. The energy level diagram and current density–voltage ( $J$ – $V$ ) curves of the devices are shown in Fig. 4, including acceptor PC<sub>61</sub>BM as the comparison group. The corresponding device characteristics with the optimal blending ratio are shown in Table 2.

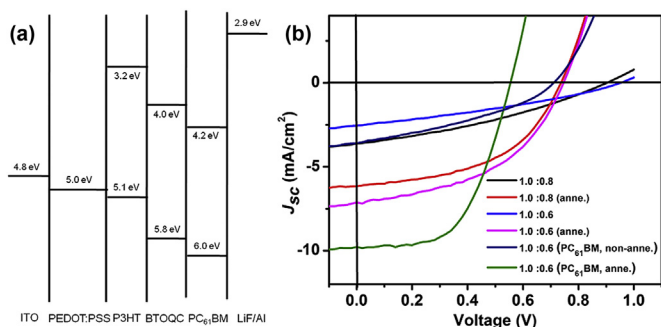


**Fig. 4.** (a) Schematic energy level diagram and (b) current density–voltage characteristics of ITO/PEDOT:PSS/P3HT:Acceptor/LiF/Al devices under illumination of AM 1.5 G, 100 mW/cm<sup>2</sup>.

**Table 2**  
Photovoltaic performance of the P3HT-based OSCs with BTOQC

Entry	Acceptor	Weigh ratio <sup>a</sup>	$V_{\text{oc}}$ (V)	$J_{\text{sc}}$ (mA/cm <sup>2</sup> )	FF	PCE (%)
1	PC <sub>61</sub> BM	1.0:0.6	0.72	3.60	0.35	0.906
2 <sup>b</sup>	PC <sub>61</sub> BM	1.0:0.6	0.56	9.78	0.56	3.04
3	BTOQC	1.0:0.6	0.96	2.55	0.317	0.777
4 <sup>b</sup>	BTOQC	1.0:0.6	0.74	7.11	0.476	2.50
5	BTOQC	1.0:0.8	0.90	3.61	0.338	1.10
6 <sup>b</sup>	BTOQC	1.0:0.8	0.74	6.17	0.492	2.24

<sup>a</sup> Weight ratio of P3HT:Acceptor.

<sup>b</sup> Annealed devices.

As shown in Table 2, the optimized device performance was achieved at weight ratio (P3HT:BTOQC) of 1.0:0.6. The compared P3HT:PC<sub>61</sub>BM device (1.0:0.6) is also included in the table for comparison (entries 1, 2). The as-cast 1.0:0.6 device that was not subjected to any heat treatment resulted in low power conversion efficiency (PCE) of 0.777% (entry 3), with open-circuit voltage ( $V_{\text{oc}}$ ) of 0.96 V, short-circuit current ( $J_{\text{sc}}$ ) of 2.55 mA/cm<sup>2</sup> and fill factor (FF) of 0.317. The effect of higher LUMO level (compared to that of PC<sub>61</sub>BM) can be seen in the high  $V_{\text{oc}}$  of the device (close to 1 V). Thermal annealing at 150 °C for 10 min significantly improved the PCE by more than threefold to 2.50% (entry 4). Similar improvement was also observed for the device with blend ratio of 1.0:0.8, although the PCE increase was only twofold (entries 5, 6). The increase in  $J_{\text{sc}}$  can be attributed to the more red-shift absorption (Fig. 1) of the blend film after the heat treatment as well as the enhancement in charge transport. Heat treatment is expected to induce self-organization of both P3HT and BTOQC molecules, resulting in more efficient charge percolation pathways for both holes and electrons.<sup>47,48</sup> The improved charge transport can be attributed to the increased FF, which suggests a decrease in device series resistance. Thermal annealing also resulted in a decrease in  $V_{\text{oc}}$  of the devices from 0.96 to 0.74 V. This possibly associates with the upward shift of P3HT HOMO level<sup>49</sup> or may be resulted from the property difference of the acceptor in the active layers. In addition, although we believe that regioisomers could have some impacts on PCE, it is impossible for us to separate these isomers with column because of their similar polarities. Due to our current limited experimental conditions, we can't give more comments on the relationship between regioisomers and their impact on PCE.

The surface morphology of the blends was investigated using tapping-mode atomic force microscopy (AFM) (Fig. 5). The height image of the non-annealed (NA) P3HT:BTOQC blend is smooth and featureless. Upon heat treatment, the blend surface becomes rougher where the root-mean-square roughness (rms) increases from 0.95 nm to 1.29 nm (Fig. S6). The surface of the non-annealed (NA) P3HT:BTOQC blend reveals the nanodomains of the active materials. After the thermal annealing (TA), these domains become

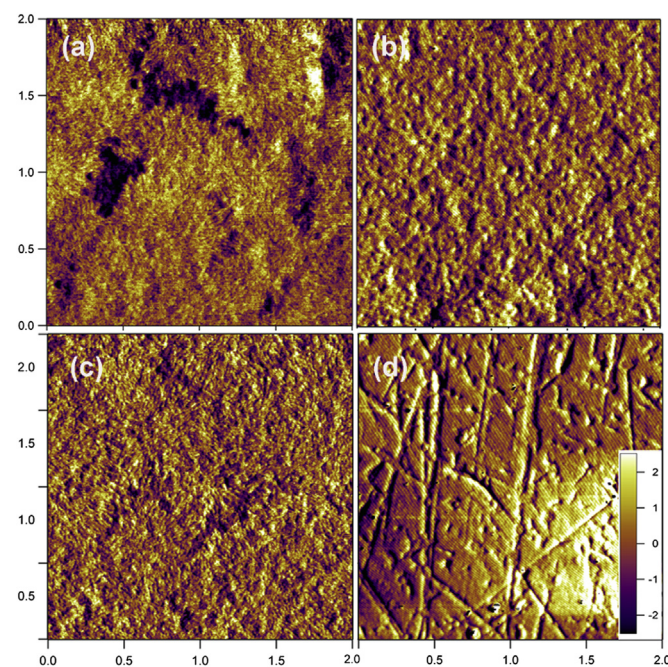


**Fig. 5.** Tapping-mode atomic force microscopy (AFM) phase images: (a, b) P3HT:BTOQC (1.0:0.6, w/w) and (c, d) P3HT:PC<sub>61</sub>BM (1.0:0.6, w/w) with (a, c) non-annealed and (b, d) thermally annealed. The scan size is 2 μm × 2 μm.

less obvious and the blend surface becomes rougher, suggesting possible domain rearrangement.<sup>50,51</sup> The presence of the fibre-like structures may contribute to the improvement in the charge transport,<sup>52</sup> which eventually increase the device performance in the thermally annealed device.

The morphology of as-cast P3HT:PC<sub>61</sub>BM blend looks similar to that of the P3HT:BTOQC. However, thermal annealing at 150 °C greatly enhanced the phase separation in the P3HT:PC<sub>61</sub>BM blend. Consequently, needle-like PC<sub>61</sub>BM crystals (which are a few microns in length) appeared in the heat-treated blend, which is common in PC<sub>61</sub>BM system. The lack of such structures in the heat-treated P3HT:BTOQC blend may account for the improvement of the device performance after thermally annealing. Nevertheless, the lackness of the ability for the P3HT:BTOQC to phase separation sufficiently could also limit its performance because the preferential interaction between BTOQC and P3HT molecules may interrupt the self-organization of both donor and acceptor molecules and, hence, lower the effectiveness of the charge transport in the device. In the next section, the charge dynamics of the P3HT:BTOQC will be discussed to further understand the interaction between the donor and acceptor.

The analysis was extended further with the fs-TAS spectra at near infrared (NIR) to probe the dynamics of the polarons, which will elucidate the behaviour of the charge transfer process from P3HT to the acceptor. The spectra at this range are shown in Fig. 6(a, b) where the polaron signal is the long lived broad signal around 1000 nm. The first few picoseconds of the signal at this NIR range is dominated by the exciton dynamics, which involves the exciton recombination from P3HT domain, germinate pairs and non germinate pairs, which will last around 100 ps.<sup>53</sup> Thus, by subtracting the pure contribution of exciton dynamics (1200 nm) from the signal at 1000 nm, we can reveal the pure polaron dynamics, which is a negative polaron in this NIR region.<sup>54</sup>

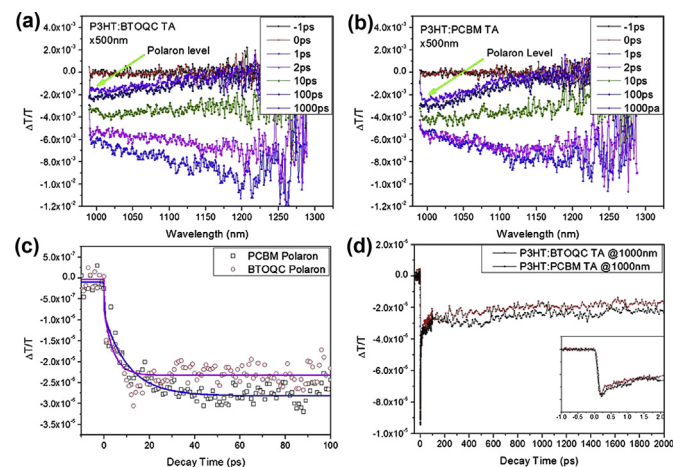


**Fig. 6.** (a, b): fs-TAS (transient absorption spectra) at near infrared region of P3HT:BTOQC (1.0:0.6, TA) and P3HT:PCBM (1.0:0.6, TA) blend sample for comparison under the same sample preparation condition; (c, d): decay profile comparison for pure polaron level between P3HT:BTOQC (1.0:0.6, TA) and P3HT:PCBM (1.0:0.6, TA) at short time scale and raw signal at 1000 nm, respectively, with an insert at first two picoseconds.

The pure polaron signal is shown in Fig. 6c where the P3HT:PCBM (1.0:0.6, TA) polaron signal has a longer rise time (10 ps) as compared to the P3HT:BTOQC (1.0:0.6, TA) (4 ps). This faster rise time may be attributed to the higher LUMO level of BTOQC than PCBM as discussed in the previous section. At longer lifetime (Fig. 6d), it can be observed that both P3HT:BTOQC (1.0:0.6, TA) and P3HT:PCBM (1.0:0.6, TA) have relatively similar polaron level and similar polaron lifetime where the BTOQC has a slightly

lower polaron signal than PCBM. This relative value indicates the number of the generated excitons, which have undergone charge separation into the acceptor side to be negative polarons.<sup>55</sup> Thus, from this relative value, it can be inferred that P3HT:BTOQC (1.0:0.6, TA) may perform slightly worse than P3HT:PCBM (1.0:0.6, TA) and it agrees with the performance result as discussed before.

### 3. Conclusion

We have successfully synthesized a new thiadiazole-*o*-quinoximethane-C<sub>60</sub> bisadducts (BTOQC), which have been explored as an acceptor in P3HT-based PSCs. This material shows device performance of 2.50% with a high  $V_{oc}$  0.74 V when the weight ratio of P3HT:BTOQC is 1.0:0.6. Although the PCE is moderate due to the phase separation, however, the benzo[2,1,3]thiadiazole is a good motif for further introduction of various functional groups. Thus, it may have great potential for further applications on optoelectronic devices based on various  $\pi$ -conjugated conducting organic materials.

## 4. Experimental section

### 4.1. Materials

All chemicals were purchased from commercial sources Sigma–Aldrich etc. and used without further purification and all solvents were purified and freshly distilled prior to use.

### 4.2. General measurement and characterization

<sup>1</sup>H NMR and <sup>13</sup>C NMR spectra were measured on Bruker DMX-300 spectrometers. Chemical shifts of NMR are reported in parts per million relative to the singlet of TMS at 0 ppm for <sup>1</sup>H NMR spectroscopy. Absorption spectra were taken on a SHIMADZU UV-2501PC UV–Vis spectrophotometer. Electrochemical cyclic voltammetry (CV) was conducted on a CHI 660C Electrochemical Workstation. In the CV measurement, a Pt disk was used as the working electrode, Pt wire as the counter electrode, and Ag/Ag<sup>+</sup> electrode (Saturated KCl solution) as the reference electrode were used in a mixed solution of *o*-dichlorobenzene: acetonitrile (5:1 v/v) with 0.1 M tetrabutylammonium hexafluorophosphate (NBu<sub>4</sub>PF<sub>6</sub>) at 100 mV s<sup>-1</sup>. The differential scanning calorimetry (DSC) analysis of fullerene derivatives was performed under a nitrogen atmosphere on an Instrument TA Q-10 at heating rates of 10 °C min<sup>-1</sup>. Tapping-mode atomic force microscopy (AFM) measurement was done with MFP-3D (Asylum Research). White light pump probe measurement was done with custom built white light pump probe (WLPP) setup. The pump laser used was generated from TOPAS (Coherent, Inc.) with laser pulse of 100 fs, repetition 1 kHz. The probe laser was generated from a fundamental wavelength of 800 nm (1 kHz) by a white light generation from a sapphire crystal with thickness of 2 mm.

### 4.3. Synthesis of BTOQC

A mixture of C<sub>60</sub> (250 mg, 0.35 mmol, 1 equiv), 5,6-bis(bromomethyl)-benzo[2,1,3]thiadiazole (**P2**, 240 mg, 0.75 mmol, 2.1 equiv to C<sub>60</sub>), potassium iodide (500 mg, 3.0 mmol, 4 equiv to bis(bromomethyl)-benzo[2,1,3]-thiadiazole), and 18-crown-6 (790 mg, 3.0 mmol, 1 equiv to potassium iodide) was dissolved in anhydrous *o*-dichlorobenzene at reflux temperature for 48 h under an argon atmosphere in dark. After cooling to room temperature, the solvent was removed under vacuum. Afterwards, the solid was transferred into methanol (10 mL×3), sonicated and centrifuged. The residual solid was purified by taking chloroform as the eluent through column chromatography on silica gel. The

separated bisadduct (regioisomers) was 122 mg, yield, 33%.  $^1\text{H NMR}$  (300 MHz,  $\text{C}_6\text{D}_4\text{Cl}_2$ )  $\delta$ : 8.35–7.89 (m, 4H), 4.96–3.89 (m, 8H), MALDI-TOF MS: calculated for  $\text{C}_{76}\text{H}_{12}\text{N}_4\text{S}_2+\text{H}^+$ , 1045.0582; found: 1045.0585 ( $\text{M}^+$ ). The solubility of BTOQC in *o*-DCB or chlorobenzene is about 15–20 mg/mL.

#### 4.4. Fabrication and characterization of OSCs

A conventional OSC structure based on ITO/PEDOT:PSS/P3HT:BTOQC/LiF/Al was used. The ITO glass was cleaned by sequential ultrasonic treatment in detergent, deionized water, acetone, and isopropyl alcohol under ultrasonication for 15 min, respectively, and subsequently dried by a nitrogen blow. Then PEDOT:PSS (poly(3,4-ethylene dioxythiophene):poly(styrene sulfonate)) (Clevios PVPAl 4083) was filtered through a 0.45  $\mu\text{m}$  filter and spin-coated at 3000 rpm for 20 s on the ITO electrode, followed by thermal annealing at 150  $^\circ\text{C}$  for 20 min. Then the substrate was transferred to an argon filled glove box. The blend solution of P3HT (10 mg/mL) and BTOQC in chlorobenzene with different weight ratio was then spin-coated on top of the PEDOT:PSS layer at 1500 rpm for 30 s. Before cathode deposition, the films were thermally annealed at 150  $^\circ\text{C}$  for 10 min. Finally, 1 nm LiF and 80 nm Al layer were deposited on the active layer under high vacuum ( $<2\times 10^{-4}$  Pa). The device active area of the OSC is ca. 4  $\text{mm}^2$ . For comparison, P3HT/PC<sub>61</sub>BM (1.0:0.6, w/w, in chlorobenzene) based solar cell with the same device structure was also fabricated. The current density–voltage ( $J$ – $V$ ) curves of the photovoltaic devices were obtained by a Keithley 2400 source-measure unit. The photocurrent was measured under simulated illumination at 100 mW/cm<sup>2</sup> AM 1.5G irradiation using a xenon-lamp-based solar simulator (Oriol 96,000 (AM 1.5G)) in an argon filled glove box. The simulator irradiance was calibrated using a certified silicon diode.

#### Acknowledgements

Q.Z. acknowledges the financial support from AcRF Tier 1 (RG 16/12) from MOE, MOE Tier 2 (ARC 20/12), CREATE program (Nanomaterials for Energy and Water Management) from NRF, and New Initiative Fund from NTU, Singapore.

#### Appendix A. Supplementary data

Supplementary data related to this article can be found at <http://dx.doi.org/10.1016/j.tet.2014.01.026>.

#### References and notes

- Günes, S.; Neugebauer, H.; Sariciftci, N. S. *Chem. Rev.* **2007**, *107*, 1324.
- Thompson, B. C.; Fréchet, J. M. J. *Angew. Chem. Int. Ed.* **2008**, *47*, 58.
- (a) Li, Y. F. *Acc. Chem. Res.* **2012**, *45*, 723; (b) Zhang, Q.; Liu, X. *Small* **2012**, *8*, 3711.
- Lin, Y. Z.; Li, Y. F.; Zhan, X. W. *Chem. Soc. Rev.* **2012**, *41*, 4245.
- Ma, W. L.; Yang, C. Y.; Gong, X.; Lee, K.; Heeger, A. J. *Adv. Funct. Mater.* **2005**, *15*, 1617.
- Li, G.; Shrotriya, V.; Huang, J.; Yao, Y.; Moriarty, T.; Emery, K.; Yang, Y. *Nat. Mater.* **2005**, *4*, 864.
- Moulé, A. J.; Meerholz, K. *Adv. Funct. Mater.* **2009**, *19*, 3028.
- Dang, M. T.; Hirsch, L.; Wantz, G.; Wuest, J. D. *Chem. Rev.* **2013**, *113*, 3734.
- Shrotriya, V.; Li, G.; Yao, Y.; Chu, C. W.; Yang, Y. *Appl. Phys. Lett.* **2006**, *88*, 073508.
- Meyer, J.; Khandavsky, R.; Görrn, P.; Kahn, A. *Adv. Mater.* **2011**, *23*, 70.
- Guo, X.; Zhang, M. J.; Tan, J. H.; Zhang, S. Q.; Huo, L. J.; Hu, W. P.; Li, Y. F.; Hou, J. H. *Adv. Mater.* **2012**, *24*, 6536.
- (a) Scharber, M. C.; Mühlbacher, D.; Koppe, M.; Denk, P.; Waldauf, C.; Heeger, A. J.; Brabec, C. J. *Adv. Mater.* **2006**, *18*, 789; (b) Zhang, Q.; Xiao, J.; Yin, Z. Y.; Duong, H. M.; Qiao, F.; Boey, F.; Hu, X.; Zhang, H.; Wudl, F. *Chem. Asian. J.* **2011**, *6*, 856.
- Price, S. C.; Stuart, A. C.; Yang, L. Q.; Zhou, H. X.; You, W. J. *Am. Chem. Soc.* **2011**, *133*, 4625.
- He, Z. C.; Zhong, C. M.; Huang, X.; Wong, W.-Y.; Wu, H. B.; Chen, L. W.; Su, S. J.; Cao, Y. *Adv. Mater.* **2011**, *23*, 4636.
- Son, H. J.; Wang, W.; Xu, T.; Liang, Y. Y.; Wu, Y. E.; Li, G.; Yu, L. P. *J. Am. Chem. Soc.* **2011**, *133*, 1885.
- Zhou, J. Y.; Wan, X. J.; Liu, Y. S.; Zuo, Y.; Li, Z.; He, G. R.; Long, G. K.; Ni, W.; Li, C. X.; Su, X. C.; Chen, Y. S. *J. Am. Chem. Soc.* **2012**, *134*, 16345.
- Small, C. E.; Chen, S.; Subbiah, J.; Amb, C. M.; Tsang, S. W.; Lai, T. H.; Reynolds, J. R.; So, F. *Nat. Photonics* **2012**, *6*, 115.
- Dou, L. T.; You, J. B.; Yang, J.; Chen, C.-C.; He, Y. J.; Murase, S.; Moriarty, T.; Emery, K.; Li, G.; Yang, Y. *Nat. Photonics* **2012**, *6*, 180.
- He, Y. J.; Li, Y. F. *Phys. Chem. Chem. Phys.* **2011**, *13*, 1970.
- Cook, S.; Ohkita, H.; Kim, Y.; Benson-Smith, J. J.; Bradley, D. C. C.; Durrant, J. R. *Chem. Phys. Lett.* **2007**, *445*, 276.
- Xie, Y.; Bao, Y.; Du, J. K.; Jiang, C. Y.; Qiao, Q. Q. *Phys. Chem. Chem. Phys.* **2012**, *14*, 10168.
- Swinnen, A.; Haeldermans, I.; vande Ven, M.; D'Haen, J.; Vanhoyland, G.; Aresu, S.; D'Olielaeager, M.; Manca, J. *Adv. Funct. Mater.* **2006**, *16*, 760.
- Zheng, L. D.; Liu, J. G.; Ding, Y.; Han, Y. C. *J. Phys. Chem. B* **2011**, *115*, 8071.
- Wienk, M. M.; Kroon, J. M.; Verhees, W. J. H.; Knol, J.; Hummelen, J. C.; van Hal, P. A.; Janssen, R. A. J. *Angew. Chem. Int. Ed.* **2003**, *42*, 3371.
- Mikroyannidis, J. A.; Kabanakis, A. N.; Sharma, S. S.; Sharma, G. D. *Adv. Funct. Mater.* **2011**, *21*, 746.
- Mikroyannidis, J. A.; Tsagkourmos, D. V.; Sharma, S. S.; Sharma, G. D. *J. Phys. Chem. C* **2011**, *115*, 7806.
- Brabec, C. J.; Cravino, A.; Meissner, D.; Sariciftci, N. S.; Fromherz, T.; Rispen, M. T.; Sanchez, L.; Hummelen, J. C. *Adv. Funct. Mater.* **2001**, *11*, 374.
- Lenes, M.; Wetzelaer, G. J. A. H.; Kooistra, F. B.; Veenstra, S. C.; Hummelen, J. C.; Blom, P. W. M. *Adv. Mater.* **2008**, *20*, 2116.
- Lenes, M.; Shelton, S. W.; Sieval, A. B.; Kronholm, D. F.; Hummelen, J. C.; Blom, P. W. M. *Adv. Funct. Mater.* **2009**, *19*, 3002.
- He, Y. J.; Chen, H. Y.; Hou, J. H.; Li, Y. F. *J. Am. Chem. Soc.* **2010**, *132*, 1377.
- Voroshazi, E.; Vasseur, K.; Aernouts, T.; Heremans, P.; Baumann, A.; Deibel, C.; Xue, X.; Herring, A. J.; Athans, A. J.; Lada, T. A.; Richter, H.; Rand, B. P. *J. Mater. Chem.* **2011**, *21*, 17345.
- Kim, K.-H.; Kang, H.; Nam, S. Y.; Jung, J.; Kim, P. S.; Cho, C.-H.; Lee, C.; Yoon, S. C.; Kim, B. J. *Chem. Mater.* **2011**, *23*, 5090.
- Cheng, Y.-J.; Liao, M.-H.; Chang, C.-Y.; Kao, W.-S.; Wu, C.-E.; Hsu, C.-S. *Chem. Mater.* **2011**, *23*, 4056.
- Zhang, C. Y.; Chen, S.; Xiao, Z.; Zuo, Q. Q.; Ding, L. M. *Org. Lett.* **2012**, *14*, 1508.
- Meng, X. Y.; Zhang, W. Q.; Tan, Z. A.; Li, Y. F.; Ma, Y. H.; Wang, T. S.; Jiang, L.; Shu, C. Y.; Wang, C. R. *Adv. Funct. Mater.* **2012**, *22*, 2187.
- Briseno, A. L.; Miao, Q.; Ling, M. M.; Reese, C.; Meng, H.; Bao, Z. N.; Wudl, F. J. *Am. Chem. Soc.* **2006**, *128*, 15576.
- Sun, Y. M.; Tan, L.; Jiang, S. D.; Qian, H. L.; Wang, Z. H.; Yan, D. W.; Di, C. G.; Wang, Y.; Wu, W. P.; Yu, G.; Yan, S. K.; Wang, C. R.; Hu, W. P.; Liu, Y. Q.; Zhu, D. B. *J. Am. Chem. Soc.* **2007**, *129*, 1882.
- Wang, X. Y.; Jiang, W.; Chen, T.; Yan, H. J.; Wang, Z. H.; Wan, L. J.; Wang, D. *Chem. Commun.* **2013**, 1829.
- Mori, T.; Nishimura, T.; Yamamoto, T.; Doi, I.; Miyazaki, E.; Osaka, I.; Takimiya, K. *J. Am. Chem. Soc.* **2013**, *135*, 13900.
- Segura, J. L.; Martín, N. *Chem. Rev.* **1999**, *99*, 3199.
- Backer, S. A.; Sivula, K.; Kavulak, D. F.; Fréchet, J. M. J. *Chem. Mater.* **2007**, *19*, 2927.
- Pilgram, K.; Zupan, M.; Skiles, R. J. *Heterocycl. Chem.* **1970**, *7*, 629.
- Neidlein, R.; Knecht, D. *Chem. Ber.* **1987**, *120*, 1593.
- Beik, P.; Gügel, A.; Spickermann, J.; Müllen, K. *Angew. Chem., Int. Ed. Engl.* **1993**, *32*, 78.
- Fernandez-Paniagua, U. M.; Illescas, B. M.; Martín, N.; Seoane, C. J. *Chem. Soc., Perkin Trans. 1* **1996**, *1*, 1077.
- Sun, Q. J.; Wang, H. Q.; Yang, C. H.; Li, Y. F. *J. Mater. Chem.* **2003**, *13*, 800.
- Lilliu, S.; Agostinelli, T.; Pires, E.; Hampton, M.; Nelson, J.; Macdonald, J. E. *Macromolecules* **2011**, *44*, 2725.
- Verploegen, E.; Mondal, R.; Bettinger, C. J.; Sok, S.; Toney, M. F.; Bao, Z. A. *Adv. Funct. Mater.* **2010**, *20*, 3519.
- Tsoi, W. C.; Spencer, S. J.; Yang, L.; Ballantyne, A. M.; Nicholson, P. G.; Turnbull, A.; Shard, A. G.; Murphy, C. E.; Bradley, D. D. C.; Nelson, J.; Kim, J.-S. *Macromolecules* **2011**, *44*, 2944.
- Yao, Y.; Hou, J. H.; Xu, Z.; Li, G.; Yang, Y. *Adv. Funct. Mater.* **2008**, *18*, 1783.
- Pivrikas, A.; Stadler, P.; Neugebauer, H.; Sariciftci, N. S. *Org. Electron.* **2008**, *9*, 775.
- van Bavel, S. S.; Barenklau, M.; de With, G.; Hoppe, H.; Loos, J. *Adv. Funct. Mater.* **2010**, *20*, 1458.
- Guo, J. M.; Ohkita, H.; Benten, H.; Ito, S. *J. Am. Chem. Soc.* **2010**, *132*, 6154.
- Guo, J. M.; Ohkita, H.; Benten, H.; Ito, S. *J. Am. Chem. Soc.* **2009**, *131*, 16869.
- Kurniawan, M.; Salim, T.; Tai, K. F.; Sun, S. Y.; Sie, E. J.; Wu, X. Y.; Yeow, E. K. L.; Huan, C. H. A.; Lam, Y. M.; Sum, T. C. *J. Phys. Chem. C* **2012**, *116*, 18015.